Accepted Manuscript online: 2021-12-02 Article published online: 2021-12-27

Sensitized Fluorescence Organic Light-Emitting Diodes with Reduced Efficiency Roll-Off

Zhiyi Li[a,b]
Ruifang Wang[a,b]
Yangyang Zeng[c]
Xiangyu Dong[a,b]
Guanhao Liu[a,b]
Xiaoxiao Hu[a,b]
Teng Gao[a,b]
Honglei Gao[a,b]
Yuanyuan Qin[a,b]
Xiuxian Gu[a,b]
Chun-Sing Lee[d]
Jiguang Liu*[c]
Pengfei Wang[a,b]
Ying Wang*[a,b]

[a] Key Laboratory of Photochemical Conversion and Optoelectronic Materials and CityU–CAS Joint Laboratory of Functional Materials and Devices, Technical Institute of Physics and Chemistry, Chinese Academy of Sciences, Beijing 100190, P. R. of China
[b] University of Chinese Academy of Sciences, Beijing 100049, P. R. of China
[c] School of Materials Design & Engineering, Beijing Institute of Fashion Technology, Beijing 100029, P. R. of China
[d] Center of Super-Diamond and Advanced Films (COSDAF), City University of Hong Kong, Hong Kong SAR, P. R. of China
* j.liu@bift.edu.cn, wangy@mail.ipc.ac.cn

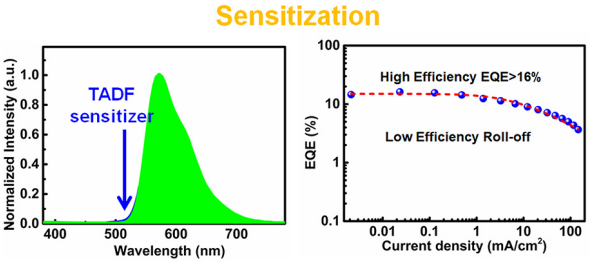

Received: 11.10.2021
Accepted after revision: 17.11.2021
DOI: 10.1055/a-1711-5768; Art ID: OM-2021-10-0041-SC

Abstract Thermally activated delayed fluorescence (TADF)-sensitized fluorescence is a promising strategy to maintain the advantage of TADF materials and fluorescent materials. Nevertheless, the delayed lifetime of the TADF sensitizer is still relatively long, which causes heavy efficiency roll-off. Here we reported a valid tactic to construct fluorescent devices with low-efficiency roll-off by utilizing the TADF sensitizer with a reduced delayed lifetime. By the construction of the sensitization system, the energy transfer efficiency can reach up to 90%. The high-energy transfer efficiency and the TADF's short delayed lifetime result in high sensitization over 95% and the maximum external quantum efficiency of 16.2%. Meanwhile, the TADF-sensitized fluorescent devices exhibit reduced efficiency roll-off with an "onset" current density of 23 mA·cm^{-2}. Our results provide an effective strategy to reduce the efficiency roll-off of the TADF sensitization system.

Key words: OLED, fluorescence, TADF

Introduction

Recently, pure organic thermally activated delayed fluorescence (TADF) materials, also known as E-type delayed fluorescence, has drawn great attention in organic electroluminescence device (OLED),[1] organic photovoltaics,[2] bioimaging,[3] and photocatalysis.[4] Through a rational molecular design strategy, TADF materials can achieve a small singlet–triplet energy gap (ΔE_{ST}).[5] For TADF materials, the lowest excited triplet state can up-convert to the lowest excited singlet state by fast reverse intersystem crossing (RISC).[6] The up-conversion needs to overcome the small ΔE_{ST} barrier. Meanwhile, the up-conversion needs electron spin-flip.[7] The TADF materials usually exhibit a relatively long delayed fluorescence lifetime.[8] The relatively long delayed fluorescence lifetime would enhance the triplet-related exciton annihilation process.[9] The triplet-related exciton annihilation process, like triplet–triplet annihilation and triplet–polaron annihilation, will cause heavy efficiency roll-off at high current density.[10] At the same time, the triplet-related exciton annihilation process will also create high-energy excitons.[11] The high-energy excitons will lead to the cleavage of chemical bonds of TADF emitters.[12] This will cause device degrada-

tion. Thus, reducing the delayed lifetime of TADF materials is meaningful for commercial applications.

It is reported that the delayed lifetime of TADF materials can be reduced in a TADF-sensitized fluorescence system.[13] In the system, it combines the advantages of the TADF molecules and the advantages of the florescent materials with the Förster resonance energy transfer (FRET) process.[14] In 2014, Adachi's group reported the first TADF-sensitized fluorescent OLED.[15] In the devices, through heavily doped TADF sensitizers, the excitons mainly formed on TADF materials.[16] The formed triplet excitons can up-convert to singlet excitons by the RISC process, thus realizing theoretically an exciton utilization efficiency of 100%.[17] Then, the FRET process from the singlet state of TADF molecules to the singlet state of fluorescent materials can occur in the system.[18] In recent years, TADF-sensitized fluorescent OLEDs have realized remarkable progress, and the device efficiency has reached up to 20%.[19] Our group reported an efficient TADF-sensitized red fluorescent device with excellent color purity. We proposed a new factor, sensitization efficiency (SE), to quantitatively evaluate the emission contribution of TADF sensitizers.[20] Subsequently, we reported a TADF-sensitized fluorescent device with low-efficiency roll-off.[21] However, the efficiency roll-off can be further reduced by reducing further the delayed lifetime of the TADF materials.

Recently, we have reported two highly efficient TADF emitters: SAT-DAC and SATX-DAC.[22] Because of their two-channel RISC process, the emitters exhibit reduced delayed lifetimes. In this work, we construct a sensitization system with SAT-DAC as the TADF sensitizer and TBRb as an orange fluorescence emitter. From SAT-DAC to TBRb, the energy transfer efficiency can reach up to 90%. Based on the sensitization system, we construct the sensitization devices. Benefitting from the high-energy transfer efficiency, the devices exhibit a maximum external quantum efficiency (EQE) of 16.2%, a current efficiency of 52.4 cd/A, a power efficiency of 45.7 lm/W, an SE of near 100% and a reduced efficiency roll-off.

Results and Discussion

To investigate the interaction between the TADF sensitizer and fluorescent materials, we measured the UV-vis absorption spectrum and photoluminescence (PL) spectrum of TBRb in solution and the PL spectrum of SAT-DAC in the doped film. As shown in Figure 1, TBRb exhibits several characteristic absorption peaks in 370–570 nm and a characteristic fluorescent spectrum centered at 569 nm. The SAT-DAC exhibits an emission spectrum at 521 nm with a full-width at half-maximum of 95 nm, which indicates its intramolecular charge transfer character. What's more, there is a wide overlap between the emission spectrum of the TADF sensitizer and the absorption spectrum of the fluorescent emitter at 450–550 nm. According to the expression for the rate constant of energy transfer (K_{ET}, see Supporting Information E1), K_{ET} is proportional to the spectral integral.[23] The broad overlap integral is beneficial to the large transfer rate constant and will facilitate the energy transfer process from the TADF material to the fluorescent material. And the Förster radius (R_0) is estimated to be 6.1 nm, which indicates the high-energy transfer efficiency.

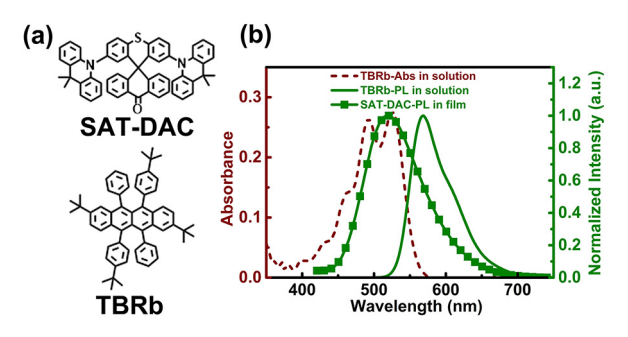

Figure 1 (a) The molecular structures of SAT-DAC and TBRb; (b) UV-vis absorption spectra and PL spectra of TBRb in solution, and PL spectra of the SAT-DAC-doped host film.

As reported earlier, a highly efficient energy transfer process can reduce the efficiency roll-off and increase the SE. To study the energy transfer process, the PL spectrum of the doped film was measured, as shown in Figure 2. For comparison, we also measured the emission spectra of the TADF sensitizer and fluorescence molecule. In the doped film, the doping concentration of SAT-DAC was kept at 40 wt% to ensure the exciton mainly formed on the TADF sensitizer. When the film was doped only with SAT-DAC, it exhibited the inherent emission of SAT-DAC. When the doping concentration of TBRb was 0.3 wt%, it exhibited two major emission peaks. One of the peaks that located at around 500 nm can be ascribed to the emission of SAT-DAC, which accounts for 18.2% of the emission spectrum. The other emission peak that dominates the emission spectrum centered at 560 nm, almost completely coinciding with the emission spectrum of TBRb. Therefore, this emission peak can be assigned to TBRb, and its emission contribution is 81.8%. With the doping concentration of TBRb raises from 0.3 to 1.0 wt%, the emission contribution of the TADF sensitizer rapidly decreases from 18.2% to 3.8%; meanwhile, the emission contribution of the fluorescent molecule increases from 81.8% to 96.2%. With the adding of TBRb in the doped film, the molecular distance (R) between SAT-DAC and TBRb diminishes. According to the relation of K_{ET} and R (as expression E2 in the Supporting Information), the sixth-order dependence of K_{ET} on R explains the huge influence of the doping concentration on the emission contribution.[24] Besides, the energy transfer efficiency (Φ_{ET}) can be expressed as: $\Phi_{ET} = 1 - \Phi_D/\Phi_D^0$.[25] Where Φ_D is the PL quantum yield (PLQY)

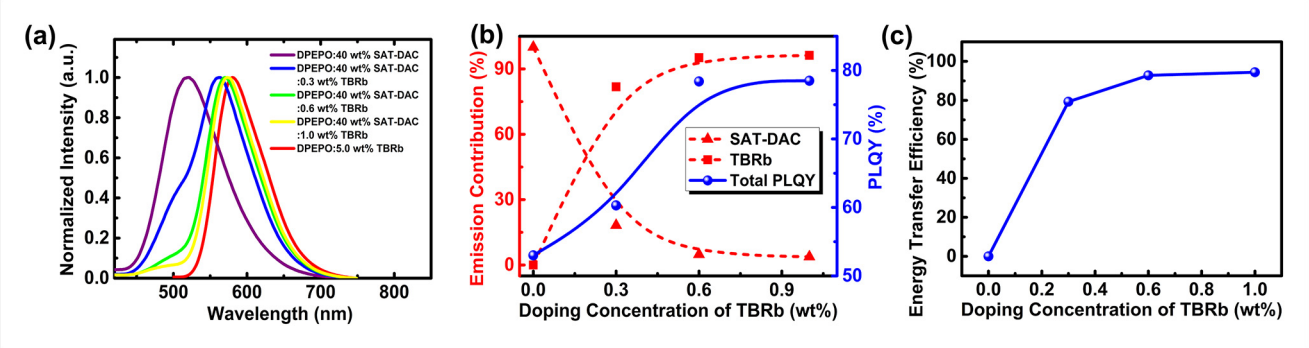

Figure 2 (a) PL spectra of the doped film with different doping concentrations; (b) emission contribution vs. doping concentration vs. PLQY characteristics; (c) the transfer efficiency of FRET between SAT-DAC and TBRb at different doping concentrations of TBRb.

of SAT-DAC in the presence of TBRb; Φ_D^0 is the PLQY of SAT-DAC in the absence of the fluorescent material. According to the varying emission contribution of SAT-DAC, Φ_{ET} was estimated to increase as the doping concentration of TBRb increased. The maximum Φ_{ET} can reach up to 90%. These results illustrate the highly effective energy transfer process from TADF sensitizers to fluorescent molecules.

To further demonstrate the TRET process, transient PL decay curves of the SAT-DAC and TBRb co-doped film was investigated, as shown in Figure 3. All the film was excited by 390 nm. To eliminate the emission of TBRb, 490 nm was chosen as the detection wavelength of the TADF sensitizer's delayed lifetime; 620 nm was selected as the detection wavelength to study the transient PL decay of TBRb. All the doped films display obvious prompt and delayed components. For the SAT-DAC-only doped film, it exhibits a distinct fluorescence lifetime of 100 ns and delayed fluorescence decay lifetime of 2.47 and 7.14 µs; both delayed lifetimes can be attributed to TADF emission. As described above, the delayed lifetime of the TADF sensitizer can be reduced by adding fluorescent materials. With the doping concentration of TBRb increased from 0.3 to 1.0 wt%, the delayed lifetime decreased from 1.72 and 5.35 µs to 0.62 and 2.39 µs, respectively. The average number of excited-state cycles (N) before the photon emission or nonradiative decay can be written as $N = \Phi_{DF}/\Phi_{PF}$. The N decreases from 469 to 25 as the doping concentration of TBRb increases from 0 to 1.0 wt%. According to the expression of delayed lifetime τ_{DF} (see Supporting Information E3),[26] both τ_{DF} and N decrease with the increase of the doping concentration, which indicates that the decrease in τ_{DF} can be vested in the suppression of the triplet formation of SAT-DAC after excitation. In addition, the PL decay at 620 nm, which corresponds to the emission of TBRb, also exhibits two components. With the increase of TBRb's doping ratio, the delayed lifetime also decreases from 1.06 and 4.37 µs to 0.35 and 1.60 µs. The trend is consistent with that of SAT-DAC. These results can demonstrate that the delayed component of TBRb originated from the energy transfer from the TADF sensitizer.

The highly efficient FRET process motivates us to evaluate the device performance of the sensitization system. Based on the sensitization system, we fabricated TADF-sensitized OLED devices with the device structure as the following: ITO/TAPC (30 nm)/mCP (10 nm)/DPEPO: 40 wt% SAT-DAC: x wt% TBRb (20 nm)/DPEPO (10 nm)/TmPyPB (30 nm)/LiF (1.1 nm)/Al (100 nm), when x = 0.5, 1.0 and 2.0, the device

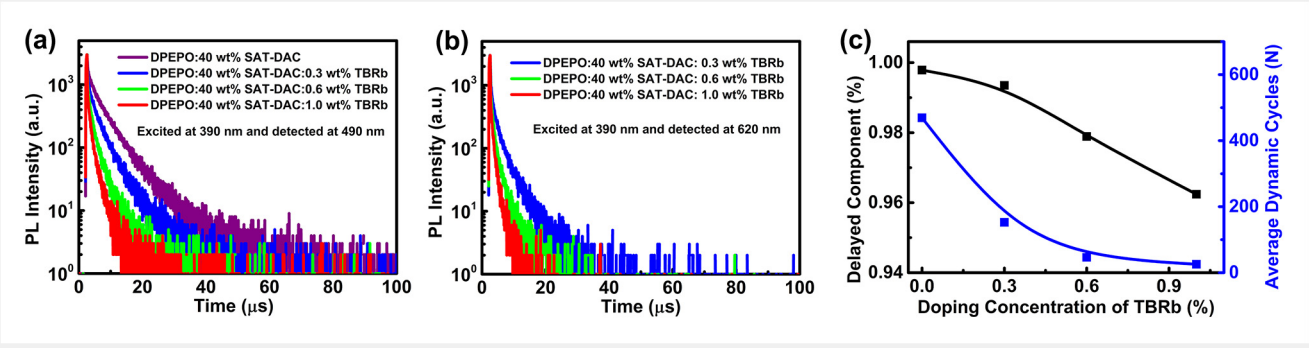

Figure 3 Transient PL decay curves of the doped films at (a) 490 nm and (b) 620 nm. (c) Delayed lifetimes of TBRb and SAT-DAC and average dynamic cycles of SAT-DAC at different doping concentrations of TBRb.

donated as **F1, F2** and **F3**.[27] For comparison, we also fabricated the fluorescent device **F4** as the control device, which has the emission layer structure of DPEPO:5 wt% TBRb (20 nm). As expected, the fluorescent device displays a turn-on voltage of 3.1 V and a maximum EQE of 4.7%. Due to the exciton formed on TBRb, the fluorescent device shows low turn-on voltage and device performance. As shown in Figure 4, all the sensitization devices exhibit TBRb-dominant electroluminescence (EL) characteristics. Compared with the EL spectrum of **F4**, only very weak emission of TADF sensitizers can be observed in the EL spectra of **F1**–**F3**. Significantly, all the sensitization devices exhibit a maximum EQE over 10%, which exceeds the limitation of traditional fluorescent devices with an EQE of 5% without light out-coupling technique.[28]

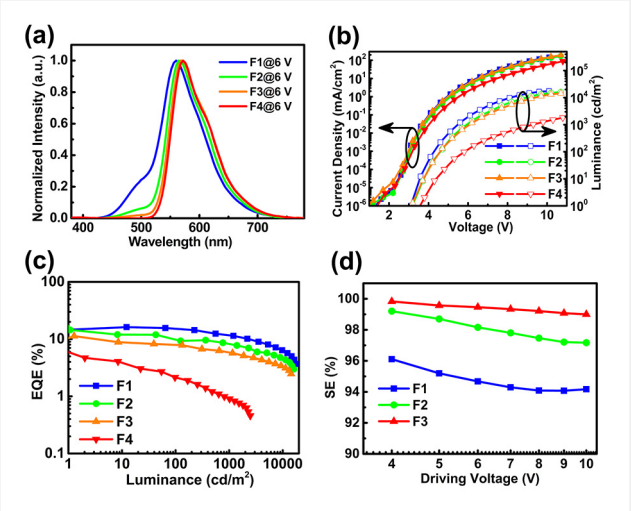

Figure 4 (a) EL spectra of all the devices at 6 V; (b) current density–voltage–luminance curves; (c) EQE–luminance curves; (d) sensitization efficiency–driving voltage curves.

Notably, the EL spectra of device **F1** overlap well with the pure EL spectrum of TBRb. According to our reported work, the SE was estimated to be as high as 96% at turn-on voltage and 94% at high driving voltage. And the SE can reach up to nearly 100% for device **F3**. Notably, from **F1** to **F3**, the maximum EQE decreases with the doping concentration of TBRb increases; while, the turn-on voltage and SE increase at higher doping concentrations. At a higher doping concentration of TBRb, energy transfer reaches higher efficiency and SE, as described earlier. However, the more excitons formed on fluorescent molecules caused lower EQE and higher turn-on voltage. Among all of the devices, device **F1** shows the highest efficiency with a maximum EQE, current efficiency, power efficiency and turn-on voltage of 16.2%, 52.4 cd/A, 45.7 lm/W and 3.1 V, respectively. Meanwhile, the device still manifested an EQE of 11.4% at the luminance of 1000 cd/m^2. The EQE of **F1** as a function of current density was fitted according to the triplet–triplet annihilation mechanism (Supporting Information E4).[29] The value of J_0 can be used as an indicator of efficiency roll-off. Benefiting from the high-energy transfer process and the reduced delayed lifetime of the TADF sensitizer in the sensitization system, the J_0 can reach up to 23.7 mA/cm^2, which reveals the low efficiency roll-off of the device. These results demonstrate that the key role of shortening the delayed lifetime in reducing the efficiency roll-off.

Conclusions

In conclusion, we demonstrate an effective strategy to reduce the efficiency roll-off of TADF-sensitized fluorescent devices. We construct a sensitization system by utilizing SAT-DAC, which has a short delayed lifetime, as the TADF sensitizer and TBRb as the fluorescence emitter. The energy transfer process was proved by the steady and transient PL spectra. The sensitization system shows a high energy transfer efficiency up to 90% and a PLQY of over 75%. Based on the sensitization system, the optimized devices exhibit a maximum EQE, current efficiency, power efficiency and turn-on voltage of 16.2%, 52.4 cd/A, 45.7 lm/W and 3.1 V, respectively. Meanwhile, the devices reveal a SE over 95% and a reduced efficiency roll-off. Our results illustrate that the efficiency roll-off of sensitized devices can be reduced by the delayed lifetime of TADF sensitizers. These results provide new perspectives to reduce the device efficiency roll-off of both TADF and fluorescent materials.

Funding Information

This work was financially supported by the National Science Foundation of China (Grant No. 9183304, 61420106002, and 21772209), the National Key Research and Development Project (No. 2017YFA0204502 and 2016YFB0401004), and the National Program for Support of Top-notch Young Professionals.

Acknowledgements

We thank Dr. H. Lu for the help in transient PL measurements.

Supporting Information

Supporting Information for this article is available online at https://doi.org/10.1055/a-1711-5768.

Conflict of Interest

The authors declare no conflict of interest.

References and Notes

(1) (a) Uoyama, H.; Goushi, K.; Shizu, K.; Nomura, H.; Adachi, C.; *Nature* **2012**, *492*, 234; (b) Jeon, S. O.; Lee, K. H.; Kim, J. S.; Ihn, S.-G.; Chung, Y. S.; Kim, J. W.; Lee, H.; Kim, S.; Choi, H.; Lee, J. Y. *Nat. Photonics* **2021**, *15*, 208.
(2) Wang, Z.; Wang, R.; Mi, Y.; Lu, K.; Liu, Y.; Yang, C.; Zhang, J.; Liu, X.; Wang, Y.; Shuai, Z.; Wei, Z. *Chem. Mater.* **2021**, *33*, 4578.
(3) Qi, S.; Kim, S.; Nguyen, V.-N.; Kim, Y.; Niu, G.; Kim, G.; Kim, S.-J.; Park, S.; Yoon, J. *ACS Appl. Mater. Interfaces* **2020**, *12*, 51293.
(4) Bryden, M. A.; Zysman-Colman, E. *Chem. Soc. Rev.* **2021**, *50*, 7587.
(5) Zhang, Q.; Li, J.; Shizu, K.; Huang, S.; Hirata, S.; Miyazaki, H.; Adachi, C. *J. Am. Chem. Soc.* **2012**, *134*, 14706.
(6) (a) Wang, H.; Xie, L.; Peng, Q.; Meng, L.; Wang, Y.; Yi, Y.; Wang, P. *Adv. Mater.* **2014**, *26*, 5198; (b) Cai, X.; Qiao, Z.; Li, M.; Wu, X.; He, Y.; Jiang, X.; Cao, Y.; Su, S. J. *Angew. Chem. Int. Ed.* **2019**, *58*, 13522.
(7) (a) Tao, Y.; Yuan, K.; Chen, T.; Xu, P.; Li, H.; Chen, R.; Zheng, C.; Zhang, L.; Huang, W. *Adv. Mater.* **2014**, *26*, 7931; (b) Wong, M. Y.; Zysman-Colman, E. *Adv. Mater.* **2017**, *29,* 1605444; (c) Wada, Y.; Nakagawa, H.; Matsumoto, S.; Wakisaka, Y.; Kaji, H. *Nat. Photonics* **2020**, *14*, 643.
(8) Li, M.; Li, S.-H.; Zhang, D.; Cai, M.; Duan, L.; Fung, M.-K.; Chen, C.-F. *Angew. Chem. Int. Ed.* **2018**, *57*, 2889.
(9) Murawski, C.; Leo, K.; Gather, M. C. *Adv. Mater.* **2013**, *25*, 6801.
(10) Reineke, S.; Walzer, K.; Leo, K. *Phys. Rev. B: Condens. Matter* **2007**, *75*, 125328.
(11) Cui, L.-S.; Ruan, S.-B.; Bencheikh, F.; Nagata, R.; Zhang, L.; Inada, K.; Nakanotani, H.; Liao, L.-S.; Adachi, C. *Nat. Commun.* **2017**, *8*, 2250.
(12) Cui, L.-S.; Ruan, S.-B.; Bencheikh, F.; Nagata, R.; Zhang, L.; Inada, K.; Nakanotani, H.; Liao, L.-S.; Adachi, C. *Nat. Commun.* **2017**, *8*, 2250.
(13) Byeon, S. Y.; Lee, D. R.; Yook, K. S.; Lee, J. Y. *Adv. Mater.* **2019**, *31*, 1803714.
(14) Chan, C.-Y.; Tanaka, M.; Lee, Y.-T.; Wong, Y.-W.; Nakanotani, H.; Hatakeyama, T.; Adachi, C. *Nat. Photonics* **2021**, *15*, 203.
(15) Nakanotani, H.; Higuchi, T.; Furukawa, T.; Masui, K.; Morimoto, K.; Numata, M.; Tanaka, H.; Sagara, Y.; Yasuda, T.; Adachi, C. *Nat. Commun.* **2014**, *5*, 4016.
(16) Kim, J. H.; Lee, K. H.; Lee, J. Y. *J. Mater. Chem. C* **2020**, *8,* 5265.
(17) Heimel, P.; Mondal, A.; May, F.; Kowalsky, W.; Lennartz, C.; Andrienko, D.; Lovrincic, R. *Nat. Commun.* **2018**, *9*, 4990.
(18) Zhang, D.; Song, X.; Cai, M.; Duan, L. *Adv. Mater.* **2018**, *30*, 1705250.
(19) (a) Song, X.; Zhang, D.; Lu, Y.; Yin, C.; Duan, L. *Adv. Mater.* **2019**, *31*, 1901923; (b) Kim, J. H.; Lee, K. H.; Lee, J. Y. *Chem. Eur. J.* **2019**, *25*, 9060.
(20) Li, Z.; Hu, X.; Liu, G.; Tian, L.; Gao, H.; Dong, X.; Gao, T.; Cao, M.; Lee, C.-S.; Wang, P.; Wang, Y. *J. Phys. Chem. C* **2021**, *125*, 1980.
(21) Li, Z.; Dong, X.; Liu, G.; Tian, L.; Hu, X.; Gao, T.; Gao, H.; Qin, Y.; Gu, X.; Lee, C.-S.; Wang, P.; Wang, Y.; Liu, Y. *Energy Fuels* **2021**, *35*, 19104.
(22) Wang, R.; Li, Z.; Hu, T.; Tian, L.; Hu, X.; Liu, S.; Cao, C.; Zhu, Z.-L.; Tan, J.-H.; Yi, Y.; Wang, P.; Lee, C.-S.; Wang, Y. *ACS Appl. Mater. Interfaces* **2021**, *13*, 49066.
(23) Wei, P.; Zhang, D.; Duan, L. *Adv. Funct. Mater.* **2020**, *30*, 1907083.
(24) Wang, H.; Meng, L.; Shen, X.; Wei, X.; Zheng, X.; Lv, X.; Yi, Y.; Wang, Y.; Wang, P. *Adv. Mater.* **2015**, *27*, 4041.
(25) Furukawa, T.; Nakanotani, H.; Inoue, M.; Adachi, C. *Sci. Rep.* **2015**, *5*, 8429.
(26) Baleizão, C.; Berberan-Santos, M. N.; *Ann. N. Y. Acad. Sci.* **2008**, *1130*, 224.
(27) OLEDs were fabricated on glass substrates precoated with 150 nm ITO. The substrates should be cleaned with detergent, ultrasonicated in water, acetone and ethyl alcohol, and subsequently dried at 75 °C (10 min) in an oven. Afterward, the substrates were exposed to oxygen plasma (10 min) in order to remove organic residues and improve the work function of ITO. Then the substrates were transferred to a thermal evaporation chamber with a pressure lower than 5×10^{-4} Pa for organic semiconductor layers and metal cathode deposition. The devices were fabricated by evaporating organic materials onto the substrate at a rate of 1–2 Å s^{-1} while LiF at a rate of 0.05 Å s^{-1} and Al metal through a rate of 5 Å s^{-1}. The pixel sizes of each OLED are 0.09 cm^2. The electroluminescence (EL) spectra were measured by a Spectrascan PR655 photometer. The current–voltage–brightness characteristics were measured by using a computer-controlled Keithley source measurement unit (Keithley 2400) with a Konica Minolta CS-200 luminance-meter under dark and ambient atmosphere. External quantum efficiencies (EQEs; %), current efficiencies (cd A^{-1}) and power efficiencies (lm W^{-1}) were calculated from the electrical and optical properties. For this calculation, we assumed Lambertian light distribution.
(28) Jung, H.; Kang, S.; Lee, H.; Yu, Y.-J.; Jeong, J. H.; Song, J.; Jeon, Y.; Park, J. *ACS Appl. Mater. Interfaces* **2018**, *10*, 30022.
(29) Baldo, M. A.; Adachi, C.; Forrest, S. R. *Phys. Rev. B: Condens. Matter* **2000**, *62*, 10967.